PHOTOSYNTHETICA
International Journal for Photosynthesis Research

DOI 10.32615/ps.2025.015 PHOTOSYNTHETICA 63 (2): 129-139, 2025

Green manure can be an auxiliary factor against dynamic photoinhibition in *Dalbergia ecastophyllum* (L.) young trees in areas impacted by mining

M.M. MENDES[*,+], I.F. RIBEIRO[*], V.F.D. SANTOS[**], F.R. PIRES[*], A.A. FERNANDES[*], L.F.T.D. MENEZES[*], R. BONOMO[*], D. CASSOL[***], J.P.R. MARTINS[****], and A.R. FALQUETO[*]

Department of Agrarian and Biological Sciences, Federal University of Espírito Santo, 29932-540 São Mateus, ES, Brazil[*]
Department of Entomology, Federal University of Viçosa, 36570-900 Viçosa, Minas Gerais, Brazil[**]
Joint Genome Institute, Lawrence Berkeley National Lab, Berkeley, CA 94720, USA[***]
Institute of Dendrology, Polish Academy of Sciences, Parkowa 5, 62-035 Kórnik, Poland[****]

Abstract

This study evaluated the efficiency of green manure (+GM) on PSII efficiency throughout the day in *Dalbergia ecastophyllum*. The experiment was carried out in a disabled clay extraction deposit, located approximately 30 km south of São Mateus city (Espírito Santo State, Brazil). Chlorophyll (Chl) index, Chl *a* fluorescence, and plant growth were measured in the summer, after 12 months of planting. +GM improved the photochemical performance of *D. ecastophyllum*, reducing the occurrence of photoinhibition throughout the day. +GM increased the photochemical quantum yield, the probability of a photon absorbed to move beyond quinone Q_A^-, and the total Chl index, resulting in higher plant height and stem diameter (+11.7 and +2.2%, respectively). The number of active reaction centers per cross-section and the performance index of PSII values were unchanged throughout the day. Full recovery of both K and L-bands occurred at night. In contrast, plants growing with –GM had higher energy losses as heat. In conclusion, these results contribute to improving revegetation techniques, to create better conditions for the planting of native tree species in degraded areas.

Keywords: chlorophyll *a* fluorescence transient; photosynthesis; revegetation.

Highlights

- Green manure presence supports photochemical processes in *Dalbergia ecastophyllum*
- Green manure absence causes damage to PSII, resulting in photoinhibition
- *D. ecastophyllum* benefited from GM because it is a nitrogen-fixing species

Received 1 August 2024
Accepted 25 April 2025
Published online 9 June 2025

[+]Corresponding author
e-mail: marcelmerlomendes@gmail.com

Abbreviations: ABS/RC – absorption flux per active reaction center; Chl *a* – chlorophyll *a*; Chl*a*F – chlorophyll *a* fluorescence; Chl *b* – chlorophyll *b*; Chl total – total chlorophyll index; DI_0/RC – total energy dissipated as heat per active reaction center; ET_0/RC – electron flux transported by active reaction center; F_0 – minimum fluorescence; F_J – fluorescence intensity at 2 ms; F_I – fluorescence intensity at 30 ms; F_K – fluorescence intensity at 0.3 ms; F_P – maximum fluorescence intensity at 300 ms; F_m – maximum fluorescence; F_v/F_0 – maximum efficiency of the photochemical process in PSII; +GM – green manure presence; –GM – green manure absence; OEC – oxygen-evolving complex; PCA – principal component analysis; PI_{ABS} – performance index (potential) for energy conservation from captured excitons to electron acceptors reduction of intersystem; PQ – plastoquinone; PQH_2 – plasto-hydroquinone; RCs – reaction centers; RC/CS_0 – active Q_A^- reducing reaction centers per cross-sectional area in PSII; SUBH – subsoiling + harrowing; TR_0/RC – energy flux captured by the active reaction center; V_I – relative variable fluorescence at 30 ms (I step); V_J – relative variable fluorescence at 2 ms (J step); φD_0 – photochemical quantum yield for heat dissipation; φE_0 – quantum efficiency of electron transfer from Q_A^- to the electron transport chain beyond Q_A^-; φP_0 – maximal quantum yield of PSII photochemistry.

Acknowledgments: The authors would like to thank Petrobras for the partnership with the Federal University of Espírito Santo and for funding the project for developing technologies for the reforestation of areas degraded by the exploration of oil and natural gas ecosystems in the northern state of Espírito Santo. The authors also thank the Fund for Support to Research and Innovation of the State of Espírito Santo (FAPES) and the National Council for Scientific and Technological Development (CNPq) for the resources granted to the Laboratory of Plant Ecophysiology (LEV) where the experiment analyses were performed. This work was financed by Petrobras S.A., regulated by the National Agency of Petroleum, Natural Gas and Biofuels (ANP Resolution 05/2015).

Conflict of interest: The authors declare that they have no conflict of interest.

Introduction

Extreme weather events caused by climate change, such as changes in precipitation and temperature, as well as alterations in soil quality, can have an impact on the plant physiology, including cultivated (Mathieu *et al.* 2014, Dubey *et al.* 2018), native (Sorte *et al.* 2012, Marenco *et al.* 2014, Manea *et al.* 2016), and invasive species (Diez *et al.* 2012, Song *et al.* 2012, Yue *et al.* 2017). Studies indicate that during the last century, there was an increase in the global temperature of about 1.0–1.1°C, and the 1990s were considered the warmest decade of the last millennium (Chao and Feng 2018). Furthermore, studies suggest an increase in global temperature in about 1 and 5°C until the end of the 21st century, depending on the region (Chao and Feng 2018, Tollefson 2020). As a consequence of this temperature increase, the growth of invasive plants is improved while the growth of native plants is decreased (Chapuis *et al.* 2004, Manea *et al.* 2016).

Associated with rising temperature, the devastation of the Atlantic Forest, considered one of the 35 global biodiversity hotspots, caused by anthropic pressures over the years, has reduced the preservation areas (Mittermeier *et al.* 2005, Noss *et al.* 2015). Restoring these environments is necessary to mitigate the impacts of climate change. To accelerate the recovery of an ecosystem, it is necessary to adopt restoration practices, involving the development of efficient techniques for revegetating degraded areas (Holl 2007). The initial revegetation of an area can create ideal conditions for its complete restoration in the future (Holl and Brancalion 2020). Thus, it is crucial to understand the details of soil–plant–atmosphere interactions, especially if we focus on the efficiency of revegetation techniques since tree planting is not as simple as it may seem (Holl and Brancalion 2020). In this perspective, because the photosynthetic processes are noteworthy for their extreme sensitivity to various external stimuli, they can serve as critical indicators of the suitability of environmental conditions for individual development (Kalaji *et al.* 2016, 2018; Stirbet *et al.* 2018). Evaluation of these processes represents an excellent way of determining the efficiency of a range techniques used by revegetation of degraded areas, through the careful monitoring and assessment of the physiological status of plants in the field (Kalaji *et al.* 2018, Zavafer *et al.* 2020).

When environmental conditions are not suitable for plant growth and development, photosynthetic capacity is progressively reduced, as observed in water stress conditions (Manea *et al.* 2016, Meng *et al.* 2016, Alemu 2020), light stress (Kalaji *et al.* 2012, Pinheiro *et al.* 2019, 2023), salt stress (Cipriano *et al.* 2023), and temperature (Yue *et al.* 2017, Alemu 2020). Consequently, less excitation energy is directed to photochemical processes, and under these conditions, plants do not use all the light energy for ATP and NADPH production. The superexcitation of PSII caused by the excessive excitation energy reaching the reaction centers (RCs) can lead to their inactivation followed by temporary or permanent damage, mainly on D1 polypeptide, increasing susceptibility to photoinhibition (Faseela *et al.* 2020). According to Marenco *et al.* (2007), the degree of photoinhibition can be inferred through the decrease of maximum potential efficiency of PSII, determined by the F_v/F_m ratio (also called φP_0), where F_m represents the maximum fluorescence and F_v the difference between F_m and the initial fluorescence (F_0). Photoinhibition can be dynamic or chronic, depending on the stress intensity to which the plant is exposed (Marenco *et al.* 2007, Azevedo and Marenco 2012).

However, plants have evolved over thousands of years (Blois *et al.* 2013, Morris *et al.* 2018) and have continuously been exposed to stressful environmental conditions, such as different levels of light intensity, temperature, relative humidity, and other environmental conditions (Pinheiro *et al.* 2019), which have caused them to develop mechanisms to release absorbed energy as heat. This mechanism is a protective measure to prevent permanent damage to their leaves (Blankenship 2010). Also, plants can adjust their antenna complex size, either expanding or reducing it, to regulate the light absorption and capture to sustain photochemical processes throughout the day (Govindjee *et al.* 2010, Pinheiro *et al.* 2019). Consequently, various studies have observed that dynamic photoinhibition typically occurs during the hottest periods of the day (Marenco *et al.* 2007, Azevedo and Marenco 2012, Pinheiro *et al.* 2019, 2023).

Because photosynthesis is particularly sensitive to environmental factors, the assessments of the photosynthetic apparatus functionality are an indicator of stress in plants (Kalaji *et al.* 2016, Stirbet *et al.* 2018). The objective of this study was to evaluate the efficiency of +GM on PSII performance throughout the day in *D. ecastophyllum* (L.) Taub., a native species of the Atlantic Forest used in revegetation projects (Mendes *et al.* 2022). Additionally, the photoprotection capacity of GM on the photosynthetic apparatus of plants in response to temperature and light variations throughout the day was evaluated.

Materials and methods

Area of study and experimental design: The study was conducted in an experiment implemented in February 2018 in São Mateus, Espírito Santo State, Brazil, in a deactivated clay mining area. This area has been exploited for more than 15 years for clay extraction to establish bases for oil exploration and now it is being revegetated (Mendes *et al.* 2022). This type of anthropogenic impact reduces the natural regeneration capacity of the area, considering, for example, the high soil compaction (Canarache 1990). The region was completely covered by the Atlantic Forest that, due to local edaphoclimatic specificities, is classified as Semideciduous Seasonal Forest (Rolim *et al.* 2016). The soil of the area is classified as a dystrophic yellow-red latosol, which is typically found in the Atlantic Forest regions (Silva *et al.* 2007) and has medium to low fertility (Santos *et al.* 2018). The climate is hot and humid (classified as Aw of Köppen), with two distinct seasons: a dry period from March to August (autumn–winter) and a rainy period from September to February (spring–

summer). The average temperature is 24°C (Alvares *et al.* 2013).

The experiment was conducted in a randomized complete block design (RCBD) with 4 blocks, 4 replicates, and 24 plots occupying a total area of 720 m^2. In February 2018, the soil was chemically analyzed and corrected, which was also previously prepared through a process of subsoiling + harrowing (SUBH). Subsequently, the species were planted under two types of plots: (*1*) without green manure (–GM), and (*2*) with green manure (+GM). Data collection was performed in the summer, after 12 months of planting, in 2019. Chl index, Chl *a* fluorescence, and plant growth data were collected in the morning (between 7 and 10 h).

Collecting atmospheric data: Samples were collected throughout the day in January 2019 under a high PPFD. The PPFD, temperature, and relative air humidity were measured using 12 external data loggers (*HOBO U12*, *Onset*, Bourne, MA, USA). The devices were placed below *D. ecastophyllum* in all treatments (n = 12). The PPFD, temperature and relative air humidity were 86.6, 586.0, 597.1, 596.3, and 39.1 µmol(photon) m^{-2} s^{-1}, 26.5, 30.0, 37.7, 31.3, and 26.0°C, and 81.1, 74.8, 50.2, 66.9, and 84.6% at 07:00, 10:00, 13:00, 16:00, and 19:00 h, respectively (*see* Fig. 1S, *supplement*).

Plant material: As shown in Fig. 1, *D. ecastophyllum*, a tree species that is nitrogen-fixing, one year old, and approximately 50 cm tall was used in this study (Mendes *et al.* 2022). Also, the experiment tested GM's capacity to improve soil quality over the short, medium, and long term (Ferreira *et al.* 2016). Thus, the GM applied consisted of a mix of seeds from several leguminous, forage, and cruciferous species: *Brachiaria brizantha* (Hochst. ex A. Rich.) Stapf, *Cajanus cajan* (L.) Millsp., *Canavalia ensiformis* (L.) DC., *Crotalaria juncea* L., *Crotalaria ochroleuca* G. Don, *Mucuna pruriens* (L.) DC., *Raphanus sativus* L., *Stylosanthes* spp. (Fig. 1). Before flowering, these plants were often cut and the biomass remained deposited in the soil for decomposition and subsequent incorporation of its residues into the soil.

Photosynthetic pigment index: To evaluate photosynthetic pigments, *ClorofiLOG* (*FALKER Automação Agrícola*, Porto Alegre, Brazil) was used. The device uses photodiodes that emit three wavelengths, two in the red range, close to the absorption peak of each chlorophyll type (635 and 660 nm) and another near-infrared (880 nm). It has a lower sensor that captures the radiation transmitted by the leaves. Thus, the emission at this wavelength allows us to estimate the chlorophyll *a* (Chl *a*), chlorophyll *b* (Chl *b*), and total chlorophyll indices (Chl total). Thus, the light passing through the leaf sample reaches the receiver, which converts the light to be transmitted as an analog electrical signal. These signals are converted into numbers and used by the microprocessor to estimate the dimensionless Chl exponent (in units), proportional to the Chl *a*, *b*, and total content present in leaf samples.

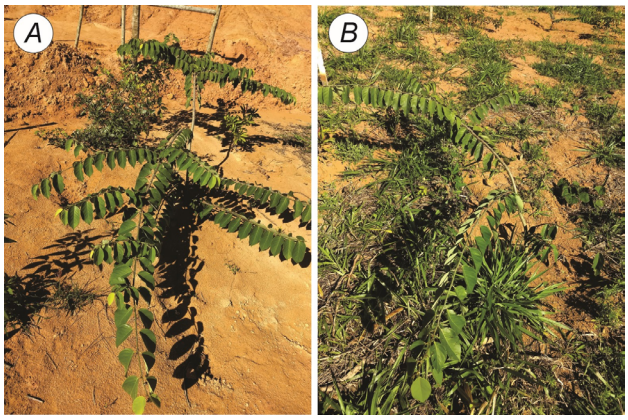

Fig. 1. *Dalbergia ecastophyllum* (L.) Taub plants. (*A*) Absence of green manure in the soil (–GM); (*B*) presence of green manure in the soil (+GM).

Chlorophyll *a* fluorescence (Chl*a*F) measurements: Chl*a*F was measured in young, undamaged, and fully expanded leaves (third or fourth leaf from the apical meristem) dark-adapted for 1 h, using leaf clips (*Hansatech*, UK) to turn the reaction centers into an "open" state (quinone A – Q_A fully oxidized). The intensity of light emitted by the device was 3,000 µmol(photon) m^{-2} s^{-1}, which was sufficient to generate maximum fluorescence in all samples (Strasser *et al.* 2004). A portable fluorometer (*Handy-PEA*, *Hanstech*, King's Lynn, Norfolk, UK) was used. Measurements were taken in one day in summer, throughout the day at 07:00 (considered as control), 10:00, 13:00, 16:00, and 19:00 h. The evaluations were performed on the same leaves throughout the day (n = 12).

The OJIP data were plotted on a logarithmic time scale from the baseline point (O) to the maximum point (P), with well-defined intermediate steps J and I. The curves were normalized between the OJ steps. The formulas used to calculate the Chl*a*F parameter were performed as reported by Stirbet and Govindjee (2011) and Strasser *et al.* (2004) as follows: V_{OK} – double-normalized Chl*a*F between O and K steps: $V_{OK} = (F_t - F_0)/(F_K - F_0)$. V_{OJ} – double-normalized variable between steps O and J steps: $V_{OJ} = (F_t - F_0)/(F_J - F_0)$. The JIP-test parameters were calculated using the formulas described by Stirbet and Govindjee (2011) and Strasser *et al.* (2004). A detailed description of parameters and their meaning can be found elsewhere, and briefly addressed in Appendix.

Plant growth traits: The plant growth was determined by measuring the plant height and stem diameter. Height was obtained by measuring the length of the aerial part, from the stem base, immediately above the ground, to the apex. The stem diameter was measured using a digital caliper. The measurements were made 3 cm above the ground.

Statistical analysis: All analyses and calculations were done with *R CRAN version 4.3.1* (*R* Core Team 2023). Non-normality and heterogeneity of variance were corrected transforming the data to logarithmic scale (for φD_0 and PI_{ABS}), square root (for TR_0/RC and DI_0/RC), and

inverse transformation (for F_0). To evaluate the differences between the treatments, the data were submitted to analysis of variance (*ANOVA*), and the significance of the differences between the mean values was determined using *Tukey*'s test at a probability level of 5%, which was performed with *agricolae version 1.3.3 R package* (Mendiburu 2023). A total of 13 variables were analyzed and plotted on radar graphics for each time of the day using *patchwork version 1.1.0* (Pedersen 2022) and *fmsb version 0.7.0 R packages* (Nakazawa 2023).

To answer the question addressed in this study, a principal component analysis (PCA) was conducted to observe the associations between the variables of Chl*a*F as a function of the presence and absence of GM as well as throughout the day. From a total of 17 variables, 14 were included in the analysis, and three variables (F_0, F_m, RC/CS_M) were excluded due to their low contribution in explaining the data. Also, growth traits and photosynthetic pigment index were excluded from this analysis. These multivariate analyses were performed using *FactoMineR version 2.3* (Lê *et al.* 2008), *factoextra version 1.0.7* (Kassambara and Mundt 2020), *ggpubr version 0.4.0* (Kassambara 2023), and *corrplot version 0.84 R packages* (Wei and Simko 2021).

Pearson's linear correlation technique was used for additional analyses, using the *corrplot package version 0.84 R* (Lê *et al.* 2008, Kassambara and Mundt 2020, Wei and Simko 2021,). To perform the correlation graphic also used *psych R package version 2.3.9* (Revelle 2023).

Results

The analysis of principal components (PCA) showed that the first two axes explained 69.5% of the total variation in the data, with axes 1 and 2 explaining 48.4 and 21.1%, respectively (Fig. 2). By observing the Chl*a*F, the photochemical parameters showed the highest correlation with axis 1 (on average, $r > 0.9$). As shown in Fig. 2*A*, these parameters (ABS/RC, TR_0/RC, ET_0/RC, DI_0/RC, V_J, V_I, φP_0, φE_0, φD_0, and PI_{ABS}) are indicators of the photosynthetic performance throughout the day. Environmental variables (temperature in °C, PPFD, and relative humidity percentage) were correlated with axis 2 (on average, $r > 0.9$) as shown in Fig. 2*A*.

The parameters related to energy losses as heat (ABS/RC, DI_0/RC, φD_0) were grouped on the right PCA side. In contrast, the parameters related to photochemical efficiency (φP_0, φE_0, and PI_{ABS}) were grouped on the left PCA side (Fig. 2*B*). Furthermore, a clear grouping of *D. ecastophyllum* individuals considering the planting method (–GM and +GM) can be observed (Fig. 2*B*). Samples growing with GM were correlated with photochemical parameters in contrast to those growing without GM, which were correlated with parameters reflecting energy losses (Fig. 2*B*).

Pearson's correlation analysis was performed between all measured parameters (Fig. 3). The relative air humidity [%], temperature [°C], and PPFD [µmol(photon) m^{-2} s^{-1}] presented a strong correlation with each other, and positively correlated with specific energy fluxes (ABS/RC, TR_0/RC, ET_0/RC, DI_0/RC), and quantum yield and efficiencies. On the other hand, relative air humidity, temperature, and PPFD were negatively correlated with the parameters related to photochemical efficiency (φP_0).

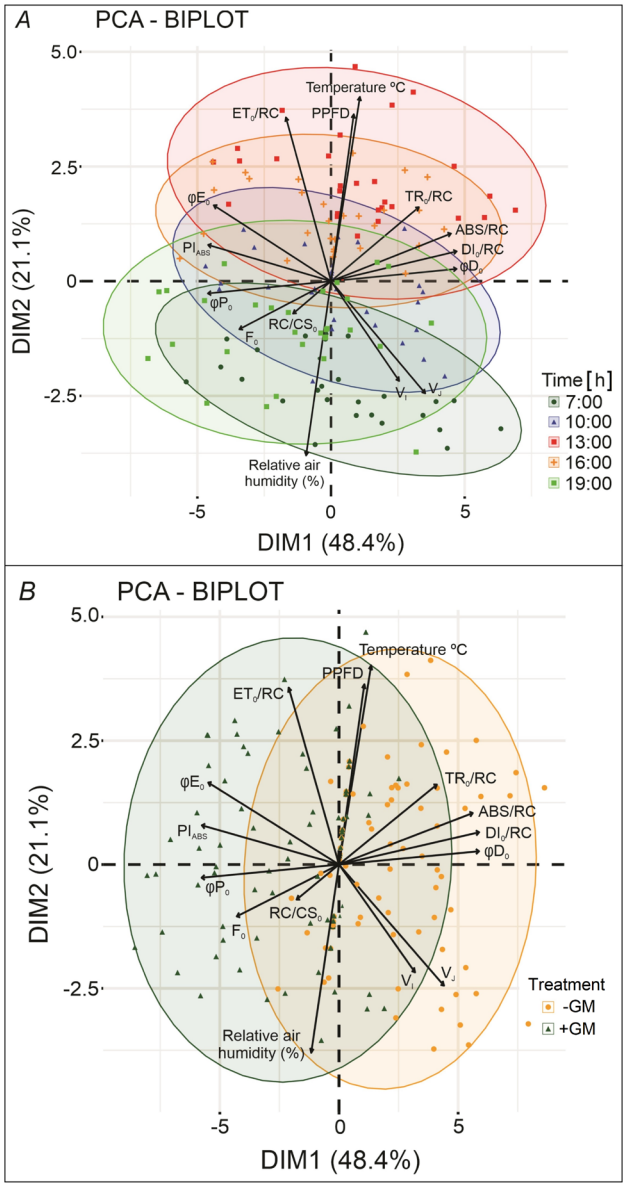

Fig. 2. Ordination produced from principal component analysis (PCA) for the parameters used in the ecophysiological evaluation of *Dalbergia ecastophyllum.* Photochemical variables [ABS/RC, TR_0/RC, ET_0/RC, DI_0/RC, φP_0, φE_0, φD_0, V_I, V_J, and PI_{ABS} (*see* Appendix)], environmental variables (relative air humidity [%], photosynthetic photon flux density – PPFD [µmol(photon) m^{-2} s^{-1}], temperature [°C]). In (*A*), the clustering is based on the time of day (7:00, 10:00, 13:00, 16:00, and 19:00 h). In (*B*), the clustering is based on the presence and absence of green manure (+GM and –GM, respectively).

The photosynthetic pigments index values were influenced by green manure (+GM). Photosynthetic pigments index differed statistically in the presence of GM. Chl total index showed an increase of approximately

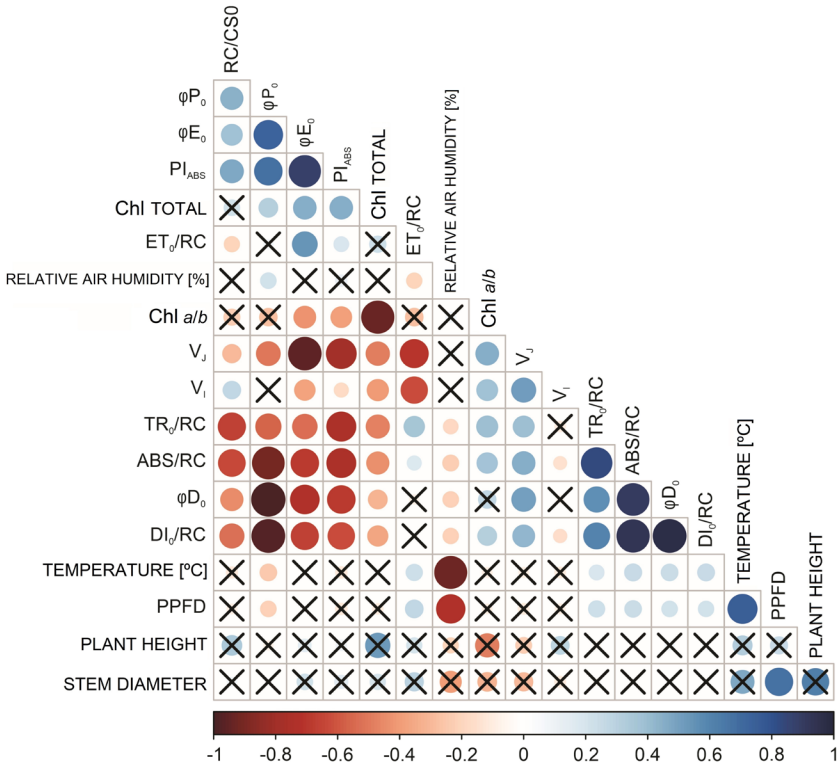

Fig. 3. *Pearson*'s correlation coefficient in *Dalbergia ecastophyllum* plants as a function of the presence and absence of green manure (+GM and –GM, respectively). *Blue symbols* indicate positive correlation while *red symbols* indicate negative correlation. ABS/RC – absorption flux per active reaction center; Chl – chlorophyll; DI_0/RC – total energy dissipated as heat per active reaction center; ET_0/RC – electron flux transported by active reaction center; PI_{ABS} – performance index (potential) for energy conservation from captured excitons to electron acceptors reduction of intersystem; PPFD – photosynthetic photon flux density; RC/CS_0 – active Q_A^- reducing reaction centers per cross-sectional area in PSII; TR_0/RC – energy flux captured by the active reaction center; V_I – relative variable fluorescence at 30 ms (I step); V_J – relative variable fluorescence at 2 ms (J step); φD_0 – photochemical quantum yield for heat dissipation; φE_0 – quantum efficiency of electron transfer from Q_A^- to the electron transport chain beyond Q_A^-; φP_0 – maximal quantum yield of PSII photochemistry.

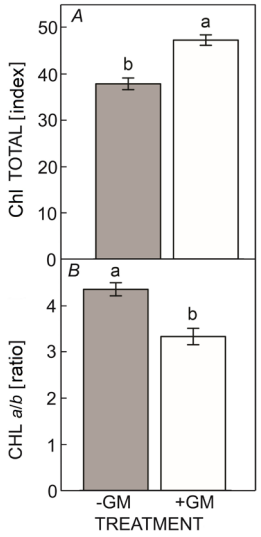

Fig. 4. Photosynthetic pigment index in *Dalbergia ecastophyllum* plants as a function of green manure (–GM or +GM). (*A*) Chl total index and (*B*) Chl *a*/*b* ratio. Among GM treatments, the means ± SEs followed by *the different letters* in each Chl index are significantly different according to *Tukey*'s test (p<0.05).

17.8%. On the other hand, Chl *a*/*b* was higher (17%) in –GM compared to those plants grown with GM (Fig. 4).

Fig. 5 shows the normalizations between the O (20 µs) and K (300 µs) steps and the O (20 µs) and J (2 ms) steps as well as their respective kinetic differences, allowing us to observe the L-band (between O and K) and the K-band (between O and J), respectively. The –GM and +GM treatments affected the functioning of the photosynthetic apparatus of *D. ecastophyllum*. In plants grown without GM, positive K (ΔV_{OJ}) and L (ΔV_{OK}) bands were observed at all times throughout the day (Fig. 5*A*,*C*). Additionally, it is possible to observe that the amplitude of the K and L-bands gradually increased and reached their maximum at 16:00 h (0.08 and 0.05, respectively). Conversely, plants grown with GM exhibited positive K (ΔV_{OJ}) and L (ΔV_{OK}) bands only during the periods of highest light and temperature (13:00 and 19:00 h). Note that the amplitudes of the L and K-bands were smaller (0.04 and 0.02, respectively) compared to those observed in plants grown without GM. The use of GM resulted in the full recovery of the K and L-bands at 19:00 h (negative amplitude of –0.02 in both K and L-bands) (Fig. 5*B*,*D*).

To better characterize the influence of GM on the *D. ecastophyllum* responses to light, the JIP-test parameters derived from the Chl*a*F curve (OJIP) were evaluated and are presented in a radar-type graph (Fig. 6). +GM increased F_0 throughout the day (Fig. 6). The values of maximum fluorescence (F_m) and the number of active reaction centers per cross-section (RC/CS_M) did not vary throughout the day. However, F_m increased in the presence of GM at 19:00 h. The values of V_J and V_I increased throughout the day in –GM, as shown in Fig. 6.

Also, –GM affected the specific energy fluxes. It was observed that ABS/RC, TR_0/RC, and DI_0/RC values were increased in –GM, while electron transportation flux (ET_0/RC) did not vary significantly (Fig. 6). Additionally, φP_0 and the probability of a photon absorbed to move beyond Q_A^- (φE_0) were higher in +GM in all the evaluations performed. On the other hand, –GM promoted significant reductions in these parameters and also increased the photochemical quantum yield for heat dissipation (φD_0) as shown in Fig. 6. Furthermore, GM was able to maintain the performance index of PSII (PI_{ABS}) on average 3 times higher than those plants cultivated in –GM conditions in all evaluations made throughout the day. Fig. 7 shows a central vertical line representing the overall mean of

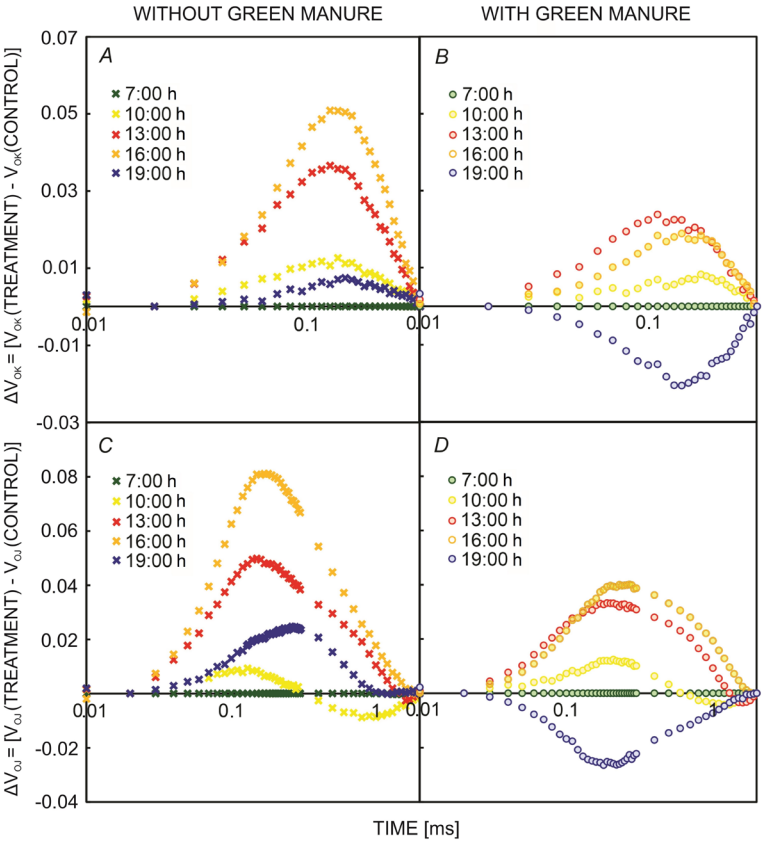

Fig. 5. K-band (0.3 ms) or ΔV_{OJ} established between 0 and 2 ms from double normalization $\Delta V_{OJ} = [V_{OJ\ (control)} - V_{OJ\ (treatment)}]$, where $V_{OJ} = (F_t - F_0)/(F_J - F_0)$ in (*A*) individuals of *Dalbergia ecastophyllum* cultivated without green manure (–GM) and (*B*) individuals of *D. ecastophyllum* cultivated with green manure (+GM). L-band (0.15 ms) or ΔV_{OK} established between 0 and 0.3 ms from double normalization $\Delta V_{OK} = [V_{OK\ (control)} - V_{OK\ (treatment)}]$, where $V_{OK} = (F_t - F_0)/(F_K - F_0)$ in (*C*) individuals of *D. ecastophyllum* cultivated in –GM and (*D*) individuals of *D. ecastophyllum* cultivated in +GM. The data were obtained throughout the day (7:00, 10:00, 13:00, 16:00, and 19:00 h).

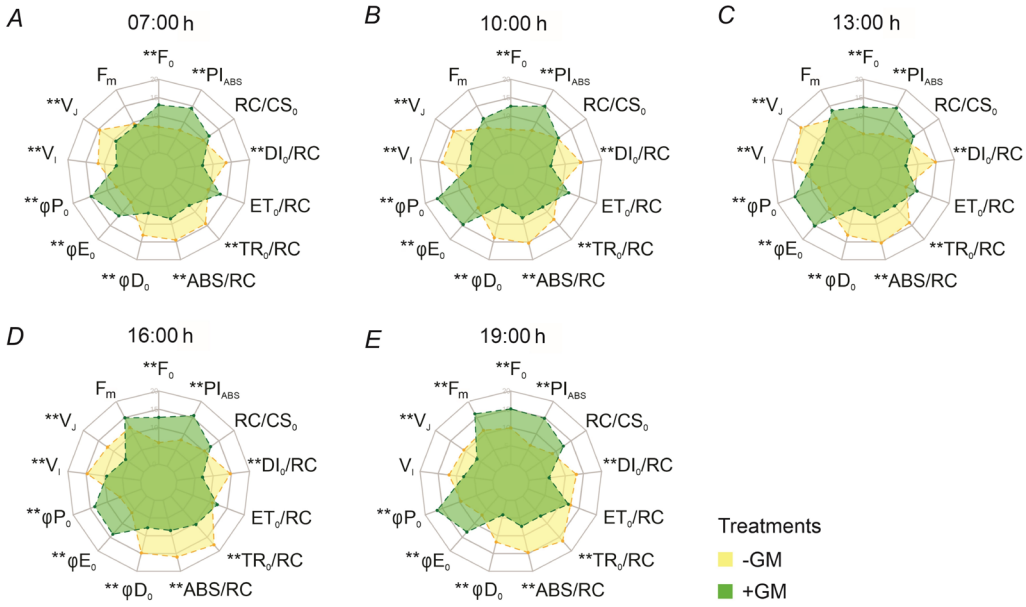

Fig. 6. JIP-test parameters considering the presence (+GM) and absence (–GM) of green manure, represented in *green* and *yellow* colors, respectively, obtained *in Dalbergia ecastophyllum* throughout the day (7:00, 10:00, 13:00, 16:00, and 19:00 h). Parameters followed by *asterisks* are significantly different according to *Tukey*'s test [** – significant at 1% probability (p<0.01); * – significant at 5% probability (p<0.05)]. ABS/RC – absorption flux per active reaction center; DI_0/RC – total energy dissipated as heat per active reaction center; ET_0/RC – electron flux transported by active reaction center; F_0 – minimum fluorescence; F_m – maximum fluorescence; PI_{ABS} – performance index (potential) for energy conservation from captured excitons to electron acceptors reduction of intersystem; RC/CS_0 – active Q_A^- reducing reaction centers per cross-sectional area in PSII; TR_0/RC – energy flux captured by the active reaction center; V_I – relative variable fluorescence at 30 ms (I step); V_J – relative variable fluorescence at 2 ms (J step); φD_0 – photochemical quantum yield for heat dissipation; φE_0 – quantum efficiency of electron transfer from Q_A^- to the electron transport chain beyond Q_A^-; φP_0 – maximal quantum yield of PSII photochemistry.

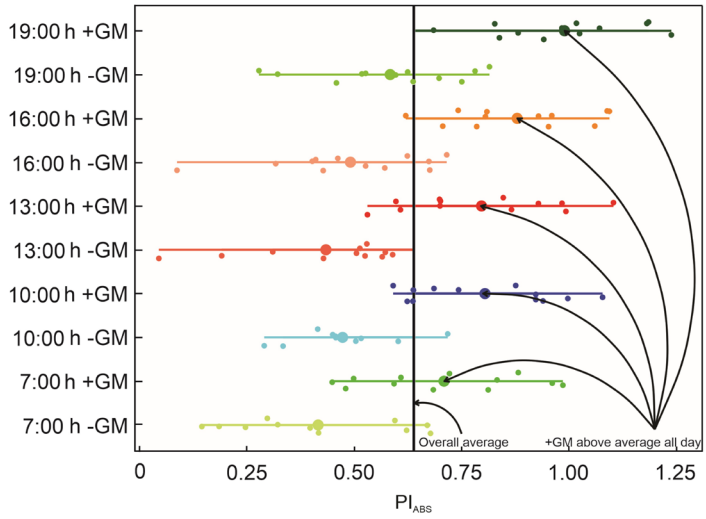

Fig. 7. Photosystem II performance index PI_{ABS} (log) in *Dalbergia ecastophyllum* plants in the presence and absence of green manure (+GM and –GM, respectively) throughout the day (7:00, 10:00, 13:00, 16:00, and 19:00 h). *The vertical line* on the graph represents the overall mean of the parameter. *The horizontal lines* represent the boxplots with the data distribution, and the mean is also represented by the larger point of each line. The means are significantly different according to *Tukey*'s test at 5% probability (p=0.05), and these points are indicated by *arrows* on the graph.

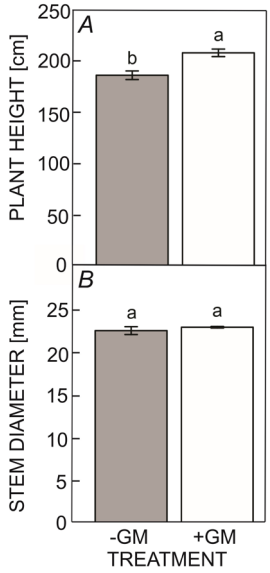

Fig. 8. Plant growth traits: (*A*) plant height [cm] and (*B*) steam diameter [mm] in *Dalbergia ecastophyllum* plants as a function of the presence and absence of green manure (+GM and –GM, respectively). Among GM treatments, the means ± SEs followed by *the different letters* are significantly different according to *Tukey*'s test (p<0.05).

this parameter considering the entire dataset, and while the PI_{ABS} mean is higher in samples collected from *D. ecastophyllum* individuals cultivated in +GM throughout the day, in individuals cultivated in –GM, the values are significantly lower and fall below the overall average for this parameter (Fig. 7).

Soil treatments also influenced the growth parameters. The plant height and stem diameter were higher in the +GM treatment (11.7 and 2.2%, respectively) (Fig. 8).

Discussion

D. ecastophyllum is a native species of the Atlantic Forest that has been studied for the revegetation of degraded areas (Mendes *et al.* 2022). This species has several ecological advantages for this purpose because *D. ecastophyllum* is a legume pioneer (Pinheiro *et al.* 2020), which has a mutualistic relationship with bacteria of the genus *Rhizobium*, capable of fixing atmospheric nitrogen. Despite its functional characteristics, it is not yet known how this species responds to different environmental conditions. In this study, light and temperature modulations were considered as factors responsible for creating adjustments in the photosynthetic apparatus to determine the conditions and resources needed for the better photosynthetic performance of this species (Kalaji *et al.* 2014, Pinheiro *et al.* 2019).

Temperature and light increase throughout the day, but the photochemical machinery adjusts to convert and/or dissipate light energy more efficiently. The PCA shown in Fig. 2*A* confirmed a clear correlation between the samples collected throughout the day with the abiotic factors analyzed. Fig. 2*A* also showed the gradual escalation of the clusters at 13:00 h (the hottest time of the day) and their correlation with PPFD and temperature, as well as the return of the last cluster at 19:00 h towards the basal part, correlated with the highest relative air humidity % found at the beginning and end of the day. Pinheiro *et al.* (2019) were also able to describe the pattern of dynamic photoinhibition of *Axonopus affinis* Chase (Poaceae) throughout the day using multivariate analysis.

When the multivariate analysis is observed (Fig. 2*B*), another type of grouping becomes evident. To *D. ecastophyllum* individuals grown in +GM conditions, the strong correlation among variables reflecting photochemical efficiency and the time of day indicated better energy use through the photochemical pathway (Li *et al.* 2018, Zavafer *et al.* 2020). On the other hand, as the temperature rises throughout the day (as shown in Fig. 2*A*), individuals grown in –GM are consistently associated with photochemical variables that indicate energy loss. This pattern reflects how plants use the excitation energy depending on the planting and also opens the way for a more detailed investigation of these differences. This approach enabled the description and comprehension of the correlations between environmental effects and patterns concerning physiological responses (Kalaji *et al.* 2018, Pinheiro *et al.* 2019, Zavafer *et al.* 2020). In this study, we used multivariate analysis because it maintains the dataset integrity and structure and is an excellent tool for visualizing hypotheses. However,

to determine the effects of dynamic photoinhibition in detail, it is necessary to analyze further the photochemical parameters that characterize this photoinhibitory condition (Pinheiro *et al.* 2019, 2023; Zavafer *et al.* 2020). Increased photosynthetic pigments index, and consequently, higher use of the energy absorbed by the photochemical pathway were recorded by Mendes *et al.* (2022) in *D. ecastophyllum* individuals cultivated with GM. These results corroborate what is observed in the multivariate analysis in Fig. 2*B*.

In plants, the photosynthetic pigments, especially Chl *b*, and several carotenoid pigments, participate in the light-capturing antenna systems (Martins *et al.* 2022). Thus, the higher Chl index observed in +GM can affect directly and positively the photosynthesis processes. However, the Chl index usually decreases under stress conditions, as previously described by Martins *et al.* (2022). High light can inhibit photosynthesis through two processes: photoinhibition and photooxidation. According to Streit *et al.* (2005), photoinhibition involves damage to RCs, especially PSII, resulting from overexcitation. The reduction of the Chl total index and the increase of the Chl *a*/*b* ratio in *D. ecastophyllum* plants grown in –GM may have reduced the photosynthetic apparatus protection against damage from excessive light.

Also, the results of this study showed that plants cultivated without GM had higher F_0 values compared to those cultivated with GM at all times evaluated. Higher F_0 indicates energetics losses in the level of light collecting complex, LHC associated with PSII (Kalaji *et al.* 2016, Sasi *et al.* 2018, Stirbet *et al.* 2018). This is due to partial inhibition of the RCs associated with PSII, which reduces the electron flow from Q_A to Q_B decreasing the use of captured energy by PSII (Goltsev *et al.* 2016, Sasi *et al.* 2018, Stirbet *et al.* 2018). Furthermore, the reductions in F_m observed throughout the day in –GM indicate a reduction of the plastoquinone (PQ) pool and electron acceptors around PSI, as commonly occurs under stress conditions (Goltsev *et al.* 2016, Kalaji *et al.* 2016). This behavior is associated with photoprotection processes through nonphotochemical dissipation (Chen *et al.* 2016, Li *et al.* 2018).

Chen *et al.* (2016) observed a correlation between the behavior of the K-band and the relative variable fluorescence at J-step (V_J) in *Ageratina adenofora* growing under thermal stress. A similar pattern was observed in this experiment (*see* Fig. 5*B–D* and Fig. 6). The higher amplitude of the K-band observed in all times evaluated in –GM is indicative of problems with the integrity of the oxygen-evolving complex (OEC), which results in a reduction in the electrons flow from water molecules until RC of PSII (Chen *et al.* 2016, Pollastrini *et al.* 2017, Kalaji *et al.* 2018). The accumulation of reduced quinone A (Q_A^-) was also significantly higher in –GM, considering the sensibility of this Chl*a*F parameter to thermal stress (Chen *et al.* 2015, Yue *et al.* 2017, Stirbet *et al.* 2018). Thus, the suppression of V_I observed in +GM treatments suggests an improvement of electron transport from $Q_A^-Q_B^{-2}$ to PQH_2 (Yusuf *et al.* 2010).

The photosynthetic electron transport chain is complex, structurally, and functionally, and many environmental factors can affect it. Interruption or delay in electron transport can overload the PSII, leading to a photoinhibition state (Li *et al.* 2018, Sasi *et al.* 2018). Photoinhibition is a response against possible temporary or permanent damage to the components of the photosynthetic electron transport chain (Kale *et al.* 2017, Stirbet *et al.* 2018). Thus, photoinhibition may be linked to the destruction and repair of the D1 polypeptide (Li *et al.* 2018, Sasi *et al.* 2018), and also to the emission of F_0. In this study, the positive amplitude of the L-band at all times evaluated in –GM treatment indicated that *D. ecastophyllum* was prone to activate photoinhibition mechanisms earlier (10:00 h) to avoid damage to the thylakoid membrane components (Kalaji *et al.* 2016, 2018; Li *et al.* 2018, Sasi *et al.* 2018). On the other hand, in individuals grown with GM, the positive amplitudes of the L-band were smaller, and at 19:00 h the L-band was negative, representing greater connectivity between the PSII units (Kalaji *et al.* 2016, 2018).

The changes in specific energy fluxes (per RC) in *D. ecastophyllum* in both –GM and +GM throughout the day can be observed in Fig. 6. Yusuf *et al.* (2010) associated increased absorption flux per reaction center (ABS/RC) values with partial inactivation of RCs. However, higher ABS/RC values may also indicate increased LHC, which supplies excitation energy to the active RCs (Yusuf *et al.* 2010, Stirbet *et al.* 2018). In the second case, the energy capture flux (TR_0/RC) follows a proportional increase in ABS/RC. In this study, it is evident that the plants growing under –GM had a significant increase in ABS/RC and TR_0/RC at all times throughout the day, as already reported by Yusuf *et al.* (2010), Zhang *et al.* (2017), and Stirbet *et al.* (2018).

Light is an environmental factor essential in photosynthesis (Murchie and Ruban 2020). However, leaves receive significantly more light than can be processed by photosynthesis (Stirbet *et al.* 2018). The data collected in this study show that the average temperature and PPDF at 13:00 h was about 37°C and 592 μmol(photon) m^{-2} s^{-1}, respectively. Therefore, the high-energy flow dissipated as heat (DI_0/RC) values observed in individuals grown under –GM is related to photoprotection processes because the superexcitation of photosynthetic electron transport chain (high ABS/RC and TR_0/RC) can cause damage to the photosynthetic membranes (Sasi *et al.* 2018). To prevent photoinhibition, *D. ecastophyllum* plants cultivated under these conditions activated this mechanism to dissipate excess absorbed energy in a controlled way *via* nonphotochemical quenching (Kale *et al.* 2017, Stirbet *et al.* 2018). Pinheiro *et al.* (2019) observed the activation of nonphotochemical processes in *Axonopus affinis* under different PPFD in pasturelands in southern Brazil.

The absence of GM promoted a significant reduction in the maximum photochemical quantum yield for primary photochemistry (φP_0) at all times evaluated throughout the day. This Chl*a*F parameter is one of the most sensitive, and the decrease observed is related to a reduction in electron transport efficiency through PSII (Zhang *et al.* 2014, 2017). The inactivation of active RCs is reflected

in the quantum yield of energy dissipation measured by φD_0 (Kalaji *et al.* 2018), reinforcing the negative effect of the absence of GM in *D. ecastophyllum*, because there was a gradual decrease of activation of RCs throughout the day. Consequently, this induces low efficiency of the photosynthetic apparatus, as verified by reduced performance index based on absorption PI_{ABS}, which represents the potential for energy conservation (Yusuf *et al.* 2010, Kalaji *et al.* 2016, Stirbet *et al.* 2018). On the other hand, the presence of GM increased the plant's ability to maintain energy flows towards photochemical activities throughout the day, as observed by the highest values obtained for φP_0, RC/CS_M, and especially for PI_{ABS} (Fig. 7). Similar results were reported by Zhori *et al*. (2015) in healthy plants of *Euphorbia cyparissias* compared to those infected by fungi (*Uromyces pisi*). This supports the premise of using these Chl*a*F parameters to evaluate the plant vitality under different stress conditions.

Plants under stress conditions may suffer blockages or damage to the photosynthetic electron transport chain. In our study, this stress condition was observed in plants growing in –GM. Canarache *et al.* (1990) affirm that soil compaction can prevent root development. In our achievement, growth traits (plant height and stem diameter) are higher in SUBH +GM in *D. ecastophyllum* (nitrogen-fixing species), most likely because this species has mycorrhizal relationships with nitrogen-fixing bacteria. In summary, besides providing photoprotection throughout the day, +GM promoted also greater plant growth.

Conclusion: In conclusion, the results of this study provide strong evidence that green manure (+GM) can improve the energy utilization in the photochemical reactions of photosynthesis, with particular emphasis on the values obtained in F_m, φP_0, and PI_{ABS}, which reflect better stability of PSII reactions. On the other hand, *D. ecastophyllum* individuals cultivated in –GM showed signs of stress and early dynamic photoinhibition (starting at 10:00 h). The GM contributes to alleviating the dynamic photoinhibition of plants grown in the field, considering that the energy losses indicating this physiological status were accentuated in –GM conditions. In addition, beneficial effects were observed on photosynthetic pigments index and plant growth. Therefore, the results of this study contribute to improving revegetation techniques, to create better conditions for the planting of native tree species of the Atlantic Forest under the stressful conditions found in the field.

References

Alemu S.T.: Photosynthesis limiting stresses under climate change scenarios and role of chlorophyll fluorescence: A review article. – Cogent Food Agric. **6**: 1785136, 2020.

Alvares C.A., Stape J.L., Sentelhas P.C. *et al.*: Köppen's climate classification map for Brazil. – Meteorol. Z. **22**: 711-728, 2013.

Azevedo G.F.C., Marenco R.A.: Growth and physiological changes in saplings of *Minquartia guianensis* and *Swietenia macrophylla* during acclimation to full sunlight. – Photosynthetica **50**: 86-94, 2012.

Blankenship R.E.: Early evolution of photosynthesis. – Plant Physiol. **154**: 434-438, 2010.

Blois J.L., Zarnetske P.L., Fitzpatrick M.C., Finnegan S.: Climate change and the past, present, and future of biotic interactions. – Science **341**: 499-504, 2013.

Canarache A.: PENETR – a generalized semi-empirical model estimating soil resistance to penetration. – Soil Till. Res. **16**: 51-70, 1990.

Cipriano R., Martins J.P.R., Conde L.T. *et al.*: Anatomical and physiological responses of *Aechmea blanchetiana* (Bromeliaceae) induced by silicon and sodium chloride stress during *in vitro* culture. – PeerJ **11**: e14624, 2023.

Diez J.M., D'Antonio C.M., Dukes J.S. *et al.*: Will extreme climatic events facilitate biological invasions? – Front. Ecol. Environ. **10**: 249-257, 2012.

Dubey A.N., Verma S., Goswami S.P., Devedee A.K.: Effect of temperature on different growth stages and physiological process of rice crop – a review. – Bull. Env. Pharmacol. Life Sci. **7**: 129-136, 2018.

Faseela P., Sinisha A.K., Brestič M., Puthur J.T.: Chlorophyll *a* fluorescence parameters as indicators of a particular abiotic stress in rice. – Photosynthetica **58**: 293-300, 2020.

Ferreira E.M., Andraus M.P., Cardoso A.A. *et al.*: [Recovery of degraded areas, green manure and water quality.] – Rev. Monogr. Ambient. **15**: 228-246, 2016. [In Portuguese]

Goltsev V.N., Kalaji H.M., Paunov M. *et al.*: Variable chlorophyll fluorescence and its use for assessing physiological condition of plant photosynthetic apparatus. – Russ. J. Plant Physiol. **63**: 869-893, 2016.

Govindjee, Kern J.F., Messinger J., Whitmarsh J.: Photosystem II. – In: Encyclopedia of Life Sciences. Pp. 15. John Wiley & Sons, Chichester 2010.

Holl K.: Oldfield vegetation succession in the Neotropics. – In: Hobbs R.J. (ed.): Old Fields: Dynamics and Restoration of Abandoned Farmland. Pp. 93-117. Island Press, Washington 2007.

Holl K.D., Brancalion P.H.S.: Tree planting is not a simple solution. – Science **368**: 580-581, 2020.

Chao Q., Feng A.: Scientific basis of climate change and its response. – Glob. Energy Interconnect. **1**: 420-427, 2018.

Chapuis J.-L., Frenot Y., Lebouvier M.: Recovery of native plant communities after eradication of rabbits from the subantarctic Kerguelen Islands, and influence of climate change. – Biol. Conserv. **117**: 167-179, 2004.

Chen Q., Guan T., Yun L. *et al.*: Online forecasting chlorophyll *a* concentrations by an auto-regressive integrated moving average model: Feasibilities and potentials. – Harmful Algae **43**: 58-65, 2015.

Chen S., Yang J., Zhang M. *et al.*: Classification and characteristics of heat tolerance in *Ageratina adenophora* populations using fast chlorophyll *a* fluorescence rise O-J-I-P. – Environ. Exp. Bot. **122**: 126-140, 2016.

Kalaji H.M., Bąba W., Gediga K. *et al.*: Chlorophyll fluorescence as a tool for nutrient status identification in rapeseed plants. – Photosynth. Res. **136**: 329-343, 2018.

Kalaji H.M., Carpentier R., Allakhverdiev S.I., Bosa K.: Fluorescence parameters as early indicators of light stress in barley. – J. Photoch. Photobio. B **112**: 1-6, 2012.

Kalaji H.M., Jajoo A., Oukarroum A. *et al.*: Chlorophyll *a* fluorescence as a tool to monitor physiological status of plants under abiotic stress conditions. – Acta Physiol. Plant. **38**: 102, 2016.

Kalaji H.M., Schansker G., Ladle R.J. *et al.*: Frequently asked questions about *in vivo* chlorophyll fluorescence: practical issues. – Photosynth. Res. **122**: 121-158, 2014.

Kale R., Hebert A.E., Frankel L.K. *et al.*: Amino acid oxidation of the D1 and D2 proteins by oxygen radicals during photoinhibition of Photosystem II. – PNAS **114**: 2988-2993, 2017.

Kassambara A.: ggpubr: 'ggplot2' Based Publication Ready Plots. *R* package version 0.6.0, 2023. *Available at*: https://CRAN.R-project.org/package=ggpubr.

Kassambara A., Mundt F.: factoextra: Extract and Visualize the Results of Multivariate Data Analyses. *R* package version 1.0.7, 2020. *Available at*: https://CRAN.R-project.org/package=factoextra.

Lê S., Josse J., Husson F.: FactoMineR: An R package for multivariate analysis. – J. Stat. Softw. **25**: 1-18, 2008.

Li L., Aro E.-M., Millar A.H.: Mechanisms of photodamage and protein turnover in photoinhibition. – Trends Plant Sci. **23**: 667-676, 2018.

Manea A., Sloane D.R., Leishman M.R.: Reductions in native grass biomass associated with drought facilitates the invasion of an exotic grass into a model grassland system. – Oecologia **181**: 175-183, 2016.

Marenco R.A., Neves T.S., Camargo M.A.B. *et al.*: [Dynamic photoinhibition of photosynthesis in canopy trees of Central Amazonia.] – Rev. Bras. Bioci. **5**: 150-152, 2007. [In Portuguese]

Marenco R.A., Antezana-Vera S.A., Gouvêa P.R.S. *et al.*: [Physiology of Amazon tree species: photosynthesis, respiration and water relations.] – Rev. Ceres **61**: 786-799, 2014. [In Portuguese]

Martins J.P.R., Wawrzyniak M.K., Ley-López J.M. *et al.*: 6-Benzylaminopurine and kinetin modulations during *in vitro* propagation of *Quercus robur* (L.): an assessment of anatomical, biochemical, and physiological profiling of shoots. – Plant Cell Tiss. Org. Cult. **151**: 149-164, 2022.

Mathieu A.-S., Lutts S., Vandoorne B. *et al.*: High temperatures limit plant growth but hasten flowering in root chicory (*Cichorium intybus*) independently of vernalisation. – J. Plant Physiol. **171**: 109-118, 2014.

Mendes M.M., Pinheiro A.C.R., Pires F.R. *et al.*: Photosynthesis and leaf traits of tree species influenced by green manure associated with soil treatments. – Commun. Soil Sci. Plant Anal. **53**: 2064-2081, 2022.

Mendiburu F.: agricolae: Statistical Procedures for Agricultural Research. *R* package version 1.3-6, 2023. *Available at*: https://CRAN.R-project.org/package=agricolae.

Meng L.L., Song J.F., Wen J. *et al.*: Effects of drought stress on fluorescence characteristics of photosystem II in leaves of *Plectranthus scutellarioides*. – Photosynthetica **54**: 414-421, 2016.

Mittermeier R.A., Fonseca G.A.B., Rylands A.B., Brandon K.: A brief history of biodiversity conservation in Brazil. – Conserv. Biol. **19**: 601-607, 2005.

Morris J.L., Puttick M.N., Clark J.W. *et al.*: The timescale of early land plant evolution. – PNAS **115**: E2274-E2283, 2018.

Murchie E.H., Ruban A.V.: Dynamic non-photochemical quenching in plants: from molecular mechanism to productivity. – Plant J. **101**: 885-896, 2020.

Nakazawa M.: fmsb: Functions for Medical Statistics Book with some Demographic Data. *R* package version 0.7.5, 2023. *Available at*: https://CRAN.R-project.org/package=fmsb.

Noss R.F., Platt W.J., Sorrie B.A. *et al.*: How global biodiversity hotspots may go unrecognized: lessons from the North American Coastal Plain. – Divers. Distrib. **21**: 236-244, 2015.

Pedersen T.: patchwork: The Composer of Plots. *R* package version 1.1.2, 2022. *Available at*: https://CRAN.R-project.org/package=patchwork.

Pinheiro A.P.B., Jardim A.S., Silva J.V.G. *et al.*: Soil preparation and NPK fertilization in the planting of five Atlantic Rainforest species in a clay extraction area. – Ciênc. Nat. **42**: e36, 2020.

Pinheiro C.L., Rosa L.M.G., Falqueto A.R.: Resilience in the functional responses of *Axonopus affinis* Chase (Poaceae) to diurnal light variation in an overgrazed grassland. – Agr. Forest Meteorol. **266-267**: 140-147, 2019.

Pinheiro C.L., Zampirollo J.B., Mendes M.M. *et al.*: Exposition of three *Cattleya* species (Orchidaceae) to full sunlight: effect on their physiological plasticity and response to changes in light conditions. – Ornam. Hortic. **29**: 57-67, 2023.

Pollastrini M., Nogales A.G., Benavides R. *et al.*: Tree diversity affects chlorophyll *a* fluorescence and other leaf traits of tree species in a boreal forest. – Tree Physiol. **37**: 199-208, 2017.

R Core Team: *R*: A language and environment for statistical computing. *R* Foundation for Statistical Computing, Vienna 2023. *Available at*: https://www.R-project.org.

Revelle W.: psych: Procedures for Psychological, Psychometric, and Personality Research. *R* package version 2.3.9, 2023. *Available at*: https://CRAN.R-project.org/package=psych.

Rolim S.G., Ivanauskas N.M., Engel V.L.: [Are the tableland forests of northern Espírito Santo ombrophilous or seasonal?] – In: Rolim S.G., Menezes L.F.T., Srbek-Araujo A.C. (ed.): [Atlantic Forest of Tabuleiro: Diversity and Endemisms at the Reserva Natural da Vale]. Pp. 47-60. Rona, Belo Horizonte 2016. [In Portuguese]

Santos H.G., Jacomine P.K.T., Anjos L.H.C. *et al.*: Brazilian Soil Classification System. Embrapa, Brasília 2018.

Sasi S., Venkatesh J., Daneshi R.F., Gururani M.A.: Photosystem II extrinsic proteins and their putative role in abiotic stress tolerance in higher plants. – Plants-Basel **7**: 100, 2018.

Silva R.C., Pereira J.M., Araújo Q.R. *et al.*: [Changes in the chemical and physical properties of a chernosol with different crop covers.] – Rev. Bras. Ciênc. Solo **31**: 101-107, 2007. [In Portuguese]

Song U., Mun S., Ho C.-H., Lee E.J.: Responses of two invasive plants under various microclimate conditions in the Seoul metropolitan region. – Environ. Manage. **49**: 1238-1246, 2012.

Sorte C.J.B., Ibáñez I., Blumenthal D.M. *et al.*: Poised to prosper? A cross-system comparison of climate change effects on native and non-native species performance. – Ecol. Lett. **16**: 261-270, 2012.

Stirbet A., Govindjee: On the relation between the Kautsky effect (chlorophyll *a* fluorescence induction) and Photosystem II: basics and applications of the OJIP fluorescence transient. – J. Photoch. Photobio. B **104**: 236-257, 2011.

Stirbet A., Lazár D., Kromdijk J., Govindjee: Chlorophyll *a* fluorescence induction: Can just a one-second measurement be used to quantify abiotic stress responses? – Photosynthetica **56**: 86-104, 2018.

Strasser R.J., Tsimilli-Michael M., Srivastava A.: Analysis of the chlorophyll *a* fluorescence transient. – In: Papageorgiou G.C., Govindjee (ed.): Chlorophyll *a* Fluorescence: A Signature of Photosynthesis. Advances in Photosynthesis and Respiration. Pp. 321-362. Springer, Dordrecht 2004.

Streit N.M., Canterle L.P., Canto M.W., Hychecki Hecktheuer L.H.: [The chlorophylls.] – Cienc. Rural **35**: 748-755, 2005. [In Portuguese]

Tollefson J.: How hot will Earth get by 2100? – Nature **580**: 443-445, 2020.

Wei T., Simko V.: *R* package 'corrplot': Visualization of a correlation matrix, Version 0.92, 2021. *Available at*: https://github.com/taiyun/corrplot.

Yue M.-F., Flory S.L., Feng L. *et al.*: Effects of extreme temperatures on the growth and photosynthesis of invasive *Bidens alba* and its native congener *B. biternata*. – Nord.

J. Bot. **35**: 377-384, 2017.
Yusuf M., Kumar D., Rajwanshi R. *et al.*: Overexpression of α-tocopherol methyl transferase gene in transgenic *Brassica juncea* plants alleviates abiotic stress: Physiological and chlorophyll *a* fluorescence measurements. – BBA-Bioenergetics **1797**: 1428-1438, 2010.
Zavafer A., Labeeuw L., Mancilla C.: Global trends of usage of chlorophyll fluorescence and projections for the next decade. – Plant Phenomics **2020**: 6293145, 2020.
Zhang L., Su F., Zhang C. *et al.*: Changes of photosynthetic behaviors and photoprotection during cell transformation and astaxanthin accumulation in *Haematococcus pluvialis* grown outdoors in tubular photobioreactors. – Int. J. Mol. Sci. **18**: 33, 2017.
Zhang M., Tang S., Huang X. *et al.*: Selenium uptake, dynamic changes in selenium content and its influence on photosynthesis and chlorophyll fluorescence in rice (*Oryza sativa* L.). – Environ. Exp. Bot. **107**: 39-45, 2014.
Zhori A., Meco M., Brandl H., Bachofen R.: *In situ* chlorophyll fluorescence kinetics as a tool to quantify effects on photosynthesis in *Euphorbia cyparissias* by a parasitic infection of the rust fungus *Uromyces pisi*. – BMC Res. Notes **8**: 698, 2015.

Appendix. Abbreviations of parameters, formulas, and description of data derived from chlorophyll *a* fluorescence according to Strasser *et al.* (2004).

Fluorescence parameters	Description
Data extracted from OJIP fluorescence transient	
F_0	Minimum fluorescence
F_K	Fluorescence intensity at the K-step (0.3 ms) of OJIP transient
F_J	Fluorescence intensity at J-step (2 ms) of OJIP transient
F_I	Fluorescence intensity at I-step (30 ms) of OJIP transient
$F_P = F_M$	Maximum fluorescence intensity at P-step of OJIP transient
Technical parameters	
$V_J = (F_{2ms} - F_0)/(F_M - F_0)$	Relative variable fluorescence at J-step (2 ms)
$V_I = (F_{30ms} - F_0)/(F_M - F_0)$	Relative variable fluorescence at I-step (30 ms)
Quantum yield and efficiencies	
$\varphi P_0 = TR_0/ABS = [1 - (F_0/F_M)] = F_V/F_M$	Maximum photochemical quantum yield for primary photochemistry
$\varphi E_0 = ET_0/ABS = [1 - (F_0/F_M)]\ \psi_0$	Quantum efficiency of electron transfer from Q_A^- to the electron transport chain beyond Q_A^-
$\varphi D_0 = 1 - \varphi P_0 = (F_0/F_M)$	Photochemical quantum yield for heat dissipation
$RC/CS_0 = (ABS/CS)\ (TR_0/ABS)\ (RC/TR_0) = F_M\ \varphi P_0\ V_J/M_0$	Active Q_A^- reducing reaction centers per cross-sectional area in PSII
Specific energy fluxes (per Q_A^- reducing reaction center of PSII)	
$ABS/RC = M_0\ (1/V_J)\ (1/\varphi P_0)$	Absorption flux per active reaction center
$TR_0/RC = M_0/V_J$	Energy flux captured by active reaction center
$ET_0/RC = (M_0/V_J)\ \psi E_0 = (M_0/V_J)\ (1 - V_J)$	Electron flux transported by active reaction center
$DI_0/RC = [(ABS/RC) - (TR_0/RC)]$	Total energy dissipated as heat per active reaction center
Performance index	
$PI_{ABS} = (RC/ABS)\ [\varphi P_0/(1 - \varphi P_0)]\ [\psi_0 - 1/\psi_0)]$	Performance index (potential) for energy conservation from captured excitons to electron acceptors reduction of intersystem